Peer-reviewed version available at *Atmosphere* **2018**, *9*, 423; doi:10.3390/atmos9110423

Medium-range probabilistic forecasts of wind power generation and ramps in Japan based on a hybrid ensemble

Masamichi Ohba, Shinji Kadokura, Daisuke Nohara

Environmental Science Research Laboratory,

Central Research Institute of Electric Power Industry

1646 Abiko, Abiko, Chiba, 270-1194, Japan

September 2018

Corresponding author: Masamichi Ohba
Central Research Institute of Electric Power Industry (CRIEPI)
Environmental Science Research Laboratory
1646 Abiko, Abiko, Chiba 270-1194, Japan
E-mail: oba-m@criepi.denken.or.jp

ABSTRACT

This study shows the application of self-organizing maps (SOMs) to probabilistic forecasts of wind power generation and ramps in Japan. SOMs are applied to atmospheric variables obtained from atmospheric reanalysis over the region, thus deriving classified weather patterns (WPs). Probabilistic relationships are established between the synoptic-scale atmospheric variables over East Japan and the generation of regionally integrated wind power in East Japan. Medium-range probabilistic wind power predictions are derived by SOM, as analog ensembles based on the WPs of the multi-center ensemble forecasts. As this analog approach handles stochastic uncertainties effectively, probabilistic wind power forecasts are rapidly generated from a very large number of forecast ensembles.

The use of a multi-model ensemble provides better results than a one-forecast model. The hybrid ensemble forecasts further improve the probabilistic predictability skill of wind power generation, as compared with non-hybrid methods. It is expected that long-term wind forecasts will provide better guidance to transmission grid operators. The advantage of this method is that it can include an interpretative analysis of meteorological factors for variations in renewable energy.

Keywords: Self-organizing maps; Weather patterns; Synoptic circulation; Multi-model ensemble; Wind power

1. Introduction

Wind energy is receiving increasing attention due to reasons ranging from climate change to its status as the fastest growing energy source globally. Global production of wind energy has significantly increased in recent decades [40]. Despite this rapid change, wind energy technology is still considered imperfect. The main factor is the fluctuation in wind energy production that can result in significant and rapid changes in power generation over a short period, known as the "ramp" phenomenon [1]. As large-scale wind energy ramp events lead to an increase in power grid instability, they must be balanced by other power sources or storage systems, such as pumped-storage hydroelectricity. Forecasting the timing of ramp events can help grid operators avoid unexpected electricity imbalances. Even with the imminent need for ramp forecasts from power grid operators, obtaining highly accurate ramp forecasts remains an important challenge from a practical point of view.

Deterministic forecasting, based on numerical weather prediction, is one of the tools that can provide useful information for decision-making by grid operators. However, imperfect boundary conditions, initial conditions, and model formulation (e.g., dynamic core, physics) result in nonlinear error propagation during model integration. To quantify forecast uncertainty, more precise knowledge of the plausible future conditions is required for decision-making. In recent decades, ensemble forecast techniques have been developed as a tool for probability forecasting to generate a set of plausible future atmospheric conditions. Medium-range (1 or 2 week) ensemble forecasts are a crucial method for reducing the social impacts of weather events. They provide significantly

more time for preparation and decision-making than short-range (i.e., a few days) forecasts. It is conceivable that probabilistic medium-range ensemble forecasts can be useful to create weekly system operation plans of electric power and then increase the capability of renewable energy ramps, adding value to power grid management by providing more confidence (and less uncertainty) than deterministic forecasts.

In addition to ensemble methods, statistical post-processing is also necessary to calibrate model output. Statistical/empirical post-processing techniques for numerical weather forecasts are frequently-used, powerful approaches that improve the impacts of model error or initial-boundary conditions. These techniques are now used in various end-user applications, including estimates of renewable energy production. A promising post-processing technique is the analog approach, in which, based on the assumption that if forecasted current (synoptic) weather conditions are similar to that in the past, such as spatial-time series of wind speed and direction, the local weather can be similar to that of the past. Several studies have explored the use of analog-based methods for producing both deterministic and probabilistic weather predictions [2,3,4,5,6,7]. Delle Monache et al. [7] showed that the analog approach is useful only to calibrate raw numerical forecasts and to generate probabilistic information from a purely deterministic forecast. Some studies have discussed the application of an analog ensemble (AnEn) to regional renewable energy forecasting [41,42].

As a very large amount of forecast data is provided in medium-range ensemble forecasts, efficient tools are required to extract useful information. The self-organizing maps (SOMs), developed by Kohonen [8], is one of the most common data mining

techniques, capable of projecting high-dimensional nonlinear features onto a visually comprehensible two-dimensional map. Attempting to overcome the problem of downscaling a large number of ensemble forecasts, recent studies [5,9,10,11] have proposed the use of a SOM-based analog technique to estimate the local weather condition from ensemble forecasts. However, no study has addressed the specific application of using SOMs for medium-range wind power forecasts.

The goal of this study is to evaluate the ability of multi-model ensemble forecasts, in combination with SOM-based analog methods, to forecast probabilities of area-integrated wind power and ramps for medium-range lead times. We applied SOMs to analyzing an area for weather patterns (WPs) over East Japan, while using the analog approach for ensemble forecasts to predict wind power generation for individual time steps over the course of up to one week ahead. This method could be categorized as a hybrid ensemble method, as suggested by Eckel and Delle Monache [19], that is skillful, compared with that based on a single deterministic forecast. This hybrid ensemble forecast (combined application of a multi-model ensemble and analog ensemble post-processing) offers relatively good prediction skill for wind power generation and its climatological/meteorological interpretation. It is implied that the application of fast techniques will increase decision-making capabilities in the user community, such as electric power transmission system operators. This study is organized as follows. Section 2 provides a description of the dataset and the methods used in this study. Section 3 shows the results of the probabilistic forecast of wind power, while examining the effects of the

multi-model ensemble in improving renewable energy predictability skill. Finally, Section 4 provides a summary of the conclusions of this study.

2. Data and method

2.1. Data

Three-hourly instantaneous values of atmospheric data for the period 1977–2010 were obtained from the Japanese 55-year Reanalysis (JRA-55) [13]. We used sea level pressure (SLP) and surface wind at 10 m. These atmospheric variables were available at a horizontal resolution of approximately 0.5°. This study focuses solely on integrated wind power generation in the Tohoku region (blue region in Fig. 1), where the production of wind-generated power is the highest in Japan. However, the time-window of wind power observation is limited to only two years (FY2011/2012, i.e., April 2011 to March 2013). In this study, we used the reconstructed wind power supply data from Ohba et al. [12], from 1977 to 2010, for training our post-process model. This wind power data is historically reconstructed using long-term observational data obtained from weather stations in Japan, called the Automated Meteorological Data Acquisition System (AMeDAS). In this study, a wind power variation that produces >30% change in wind power generation over ≤ 6 h is defined as a "wind ramp event," similar to previous study [12]. The positive and negative quick change qualifies as a "ramp up and ramp down", respectively.

2.2 Ensemble forecasts

We also used past operational medium-range ensemble forecasts from five weather prediction centers: JMA, NCEP, UKMO, CMC, and ECMWF. The ensemble forecast data for 6-hourly values of sea level pressure and surface wind at 10 m are obtained from the TIGGE (THORPEX Interactive Grand Global Ensemble) portal at ECMWF from April 2011 to March 2013. As part of the THORPEX research program, this dataset is currently available for non-commercial research purposes only at a two-day delay. The forecast length used was 216 h, while the total ensemble size was 168. Only the ensemble forecasts initialized at 12:00 UTC were used here to compare the products, while creating a multi-model (i.e., multi-forecast center) ensemble based on the data from the five weather prediction centers.

2.3 SOM technique

To establish links between various WPs and their impacts on regionally integrated wind power, artificial neural network learning mechanisms were used in this study. SOMs, developed by Kohonen [8], are one of the most commonly used nonlinear pattern recognition techniques. SOMs project high-dimensional data to a visually comprehensible two-dimensional map. Since SOMs provides a spatially organized set of patterns of data variability, this technique has already been used in many synoptic climatological analysis (readers can refer to Ohba et al. [14]). Patterns are topologically ordered across the SOM array based on pattern similarity such that the farthest point of the array contain patterns with the largest dissimilarity. As described in previous studies [15], SOMs offers many advantages for WPs analysis.

In this study, we applied SOMs to the atmospheric variables derived from JRA55 around the Tohoku region (135°E-145°E, 35°N-44°N). The SOM projects these input vectors onto regularly arranged two-dimensional arrays. Each of the arrays, referred to as a node, has one reference vector. For example, a 50 × 50 grid SOM comprises 2500 reference vectors, which project onto a map composed of 2500 nodes. The reference vector represents a generalized pattern of input vectors. For more details, refer to other recent studies [11]. To train the SOM, we used SLP, surface wind vector, and surface wind speed that showed high correlation to the wind power generation time series. We used the torus-type SOM, instead of the conventional SOM, as it has no edges in the map [16]. The SOM was applied on a three-month basis for the period 1977–2010, i.e., boreal spring (March-April-May: MAM), summer (June-July-August: JJA), fall (September-October-November: SON), and winter (December-January-February: DJF). We mainly present the winter results, during which high wind power generation are observed in Japan [12].

2.4 SOM based analog ensemble

A SOM is used in this study to estimate wind energy variation in the region by first creating a relationship between atmospheric fields and local wind power generation. Each node in SOM defines the wind power generation corresponding to each analog WP. Based on this link between the SOM-obtained WPs (represented by reference vectors) and the corresponding regionally integrated wind energy, we obtained a forecast PDF of wind power based on the atmospheric variables of the TIGGE multi-center ensemble. This can

be regarded as an alternative to conventional analog [2,3] or analog-ensemble [7] techniques presented in previous studies. While original analog-ensemble compare past forecast with past forecast, this method compares past forecast with past analysis. The SOM establishes a nonparametric relationship between predictor (WPs) and predictands (wind power), subsequently requiring some statistical assumptions. In this study, the forecast PDF is estimated using a set of past historical power generation data corresponding to the best analogs (atmospheric reanalysis) for the current multi-model ensemble forecast. The observational data for each analog is a member of the analog ensemble [7]. One advantage may be to significantly lower the computational expense by compressing the analogs using SOMs. While the original analog ensemble method [7,17] generally uses a fixed number of analogs (such as 25 in [18]), the number of analogs (i.e., number of best match) here are determined by the SOM, leading to a difference among the SOM nodes in this method. To capture the spatial-time evolution of weather patterns, ±3 h time WP (i.e., 6 h time window for the analog trend) is also included in the input vector, with all three WPs equally weighted. The predictor variables are also treated equally.

To train the SOM, the same variables are extracted from the TIGGE ensemble data for a particular region. Based on their distance from the reference vectors, each WP of the ensemble forecasts is assigned to its best-match node. 168 forecast patterns are available at 6-hour intervals. The ±3 h WPs for analog trends are obtained by linear interpolation. Finally, the predicted composited PDF is obtained from the PDF, assigning the regional wind power to each node. We used relatively large-size SOMs compared to

198 previous studies to provide greater detail in the atmospheric patterns relevant to wind
199 power variability. A schematic diagram of the algorithm of the downscaling technique is
200 shown in Fig. 2 and summarized below.

201 (1) Nine SOMs are applied to the atmospheric variables (top-left panel). 50 × 50,
202 80 × 80, 100 × 100 SOMs are used. Each SOM is trained separately with absolute
203 wind speed, wind vector, and SLP, i.e., a total of nine SOMs was used.

204 (2) PDFs of wind power generation and ramp probability are estimated (obtained
205 from observational data; bottom-left panel) for each node of (1).

206 (3) Using the SOMs obtained in (1), the node that best matches the output of the
207 multi-model ensemble forecasts (top-right panel) is selected from the SOM maps,
208 respectively.

209 (4) Wind power PDFs are derived by compositing the individual results of ensemble
210 forecasts obtained in (3) (bottom-right panel).

211 (5) The ensemble composited PDF of wind power generation for the targeted region
212 is obtained from (4).

213 The use of a 50 × 50 SOM results in a mean number of analogs of approximately 10,
214 but the 80 × 80 yielded about 4, and the 100 × 100 yielded about 2.5. We decided to use
215 three different SOM sizes since numbers of analog is important parameters of the analog
216 ensemble. This method could be regarded as a SOM-based hybrid multi-model analog
217 ensemble [11]. This analog ensemble is sensitive to the selection of parameters, such as
218 SOM dimension size and atmospheric variables. Sensitivity to the choice of input was
219 tested using other variables. The best combination obtained was used in this study. For

example, previous studies [18,17] on wind power generation suggest that wind speed and direction are important for wind power forecasts. The selection of the variables in this study is consistent with the results of previous studies.

3. Wind ramp prediction based on multi-model ensemble forecast

3.1. Estimated wind power and ramp

Generally, synoptic WPs, in relation to large-scale atmospheric conditions, are important for comprehending wind power variations, since they affect near-surface wind [20,21,22,23]. Therefore, they can be good predictors [24,25,26,27,28,39]. For example, a frontal system passage, a low-level jet, and a planetary boundary layer growth can be major factors in wind power variations [29]. Wind power ramps in Japan are mainly caused by large fluctuations in wind speed in relation to the time-evolution of synoptic circulation over East Asia [12] that always affects the load generation balance.

Since regional wind power variations can have various atmospheric origins, in addition to being nonlinearly related to various meteorological factors, the classification of synoptic-scale weather background conditions could be useful not only for understanding weather factors, but also for improving wind power forecasts. First, in this section, we present the results of a SOM-based WP classification. Three examples of WPs are presented in Fig. 3. The mean atmospheric condition corresponds to the reference vector derived from the 50 × 50 SOM analysis for SLP during DJF (i.e., the 3 h by 3 h WPs, classified into 2500 nodes). The SOM analysis uses the 24480 (8 day^{-1} × 90 days in DJF × 34 years) data as the input vector. The SLP values used here are obtained by

242 removing the regional mean SLP values from the original data at each time step. Red and
243 blue shading indicate relatively high and low SLPs, respectively. We have also showed
244 the corresponding wind power generation, ramp up and down rates, and the node-mean
245 maximum increase and decrease in wind power generation over a period ≤ 6 h
246 corresponding with each WP. The patterns are selected as representative WPs that can
247 lead to relatively strong wind power generation or ramp, consistent with the dominant
248 wind power variation patterns in Japan, as discussed in previous studies [12].

249 During winter, East Asian winter monsoons dominantly affect Japan's climate and
250 local weather conditions, which is characterized by cold air outbreaks originating from
251 the negative zonal pressure gradients between the Aleutian Low and the Siberian High.
252 Two typical cyclone tracks are observed around Japan in winter, the southern coastal
253 cyclone track and the Japan Sea cyclone track. In Fig. 3, we see the impact of WPs on the
254 regional wind power generation. Corresponding to the distribution of SLP, the regional
255 wind power generation responses to the WPs are significantly different. For example, the
256 WP at the top of Fig. 3a, in eastern Japan, is covered by a strong zonal SLP gradient. The
257 SLP gradient is very effective at stably producing wind power over the region, with
258 variations ≤ 6 h being significantly weaker. However, low pressure systems approaching
259 the region from the northwest can cause more frequent ramp-ups (Fig. 3b). A meridional
260 SLP gradient covers the Tohoku region, associated with the low-pressure system located
261 at the north of the region (Fig. 3b), which can result in a rapid increase in surface wind
262 speeds within several hours. The cold front in relation to the mid-latitude cyclone passes
263 is clearly seen. In contrast, the SLP gradient over the region shown in Fig. 3c decreases,

due to a reduction of high SLP over southwest Japan, resulting in more frequent ramp-downs. These results imply that different WPs can result in differences in wind power generation and its subsequent stability.

An example of the relationships between WPs and wind power variations (node-mean) on the SOM lattice is presented in Fig. 4a. In this figure, a relatively strong wind power generation (i.e., exceeding 0.7-0.8 p.u.) is observed in the bottom-right on the SOM. We find strong contrast between nodes. This implies that integrated wind power generation in this region is strongly dependent on synoptic WPs. The SOM analysis of wind power variability over a 6 h time zone also allows us to estimate average wind power variations. The occurrence rates of ramp-up and ramp-down events are also shown in Fig. 4a. It is clear that the nodes denoting a higher occurrence rate of ramp events are separately concentrating in the SOM, implying that both, wind power generation and ramps, are highly dependent on synoptic WPs. As denoted by Ohba et al. [12] many nodes share probability of a ramp-up/down event.

Figure 5 shows four examples of probabilistic forecasts of wind power generation (top) and ramp (bottom), obtained from the multi-model ensembles (MME) of TIGGE through SOM analysis. Gray lines represent the ensemble spread of the 50th percentile output, obtained from the multi-model ensembles, while the green shading represents the PDF of wind power generation, obtained from the hybrid (multi-model analog) ensemble method. In these cases, throughout the period, the predicted wind power generation is in close agreement with the observational result. The PDF covers the observed wind power generation well, while occasionally overestimating/underestimating the power generation.

As for the second half of the period, the predicted wind power generation generally captures the high risk of ramp events relatively well. As the best estimates (50th percentile) of each ensemble member gradually extend, they approach the climatological PDF with reductions in the day-to-day difference.

Probabilistic ramp forecasts are represented by red (ramp-up) and blue (ramp-down) dots and bars in Fig. 5. The ramp probability obtained from the SOM node is represented by a bar, which is the mean of the estimated value of 168 ensembles. The error bar indicates the maximum and minimum values in the nine SOMs. We additionally estimated the ramp probability using the 50th percentile value of each ensemble (represented by the gray line in Fig. 5), denoted by a dot. The defined ramp-up and down events seen in the observed wind power generation (i.e., actual ramp events) are represented by red and blue lines. In these cases, ramp events are forecasted some number of days before the occurrence.

Figure 4b shows the footprints of the multi-model ensembles on the SOM lattice (Fig. 4a), predicted from 31 January 2013 (corresponding to Fig. 5b). The black line box in Fig. 4b shows the actual WP seen in the SOM (i.e., the best-matching node of the reanalysis). The frequency of occurrence of each SOM pattern results from mapping 168 ensembles × 4 times (in one day) to the SOM. If the forecasts are "perfect," a very dark square is identical to the solid black box, indicating that all forecast ensembles matched the observations. The spread of the colored boxes indicates the range of skill of the ensemble members, which varies by forecast days. The frequencies of WP in the multi-model (168) ensemble extend gradually on the SOM, while forming the groups. In this

case, the multi-model ensemble forecast captures the atmospheric conditions of the actual state relatively well for forecast day eight (except for forecast day four, which could be related to an underestimation of rapid decrease in wind power in Fig. 5b). The expanse of forecasts on the SOM can be an effective way to visually grasp the broadening of ensembles and the reliability of prediction.

As an example of the inter-model difference, we also show the results of the individual forecast centers separately in Fig. 6. We find a relatively large diversity of wind power forecasts among the models. In this case, the UKMO model captures the ramp-up and down that occurred on 4 February well. However, two days later, most of the models capture both, the ramp-up (on 4 February) and down (on 5 February) well, as seen in Fig. 5c. In this case, the ensemble spread is relatively small in the UKMO and NCEP models.

3.2 Forecast skill of wind power variations

This subsection evaluates the predictability of wind power generations derived from this method, based on the ensemble forecasts for FY2011/2012. Figure 7 shows the forecasted PDF of wind power generation and ramp probability, obtained from the hybrid multi-model-analog ensemble during mid-December to January of 2012/2013. The forecasted PDF for each forecast day (2, 3, 5, and 7-day lead times) is shown separately. The green shading in this Fig. shows the obtained PDF of the wind power generation, while the dot at the bottom indicates the ramp probability. Moreover, the ramp probability obtained from the ensemble means of SOM nodes are represented by the dots and bars. The results obtained from this method show a relatively wide-range PDF. In the Tohoku

region, the predicted wind power generation by the hybrid ensemble is relatively accurate (i.e., most of the observed wind power generation is included in the 95th percentile), especially for forecast day 2. The forecast skill decreases gradually, while the extent of the PDF increases with respect to the forecast length, which could be regarded as a convergence of the PDF towards the climatological PDF. The forecast uncertainty varies substantially from day to day after forecast day 3. As for the longer range (forecast day 7), we find wide variations in the predictability/uncertainty, which is known as windows for "forecasts of opportunity" [30,31,32,33] in relation to planetary-scale teleconnections.

We have shown the root mean square error (RMSE) for each ensemble forecast between the median of the probabilistic forecast and observations (Fig. 8a) to measure the average forecast error. The ensemble forecast aims to construct the uncertainty information. As a metric of probabilistic forecast verification, we have also included the continuous ranked probability score (CRPS) [34], one of the measures of integrated squared difference of the cumulative distribution function (CDF) of the forecasts (Fig. 8b) from observations. CRPS is commonly used to assess the respective accuracy of probabilistic forecasts. The RMSE and CRPS of the wind power forecasts are shown for the multi-model and each 5 ensemble forecasts for 2-8 days' lead time. The results of CRPS and RMSE are relatively similar to each other. Both, CRPS and RMSE, show that the ECMWF ensemble forecasts have the best skill in the five models, while the UKMO has the second-best skill. The remaining models have a similar level of accuracy. The effect of combining the single-model systems can be seen in MME. The RMSE and CRPS of the MME result in lower RMSE and CRPS for all lead times.

352 In addition to the forecasts of wind power generation, we also assessed the forecast
353 of wind ramp events provided from the hybrid ensemble forecasts in probabilistic form.
354 Commonly used verification methods for probabilistic forecasts are Brier score (BS) and
355 reliability diagrams. To check the skill of the wind power forecasts, we used BS (Fig. 8c)
356 and reliability diagrams obtained from the multi- and single-center ensembles for
357 FY2011/2012. Figure 9 presents the reliability diagrams for probabilistic forecasts of
358 wind power ramps over the region for that period. The centers of circles in the upper-left
359 and lower-right of the diagonal line indicate underestimation and overestimation of the
360 risks, respectively. Most of the single-center ensemble forecasts tend to overestimate the
361 risks, even with a lead forecast time of two days. The MME forecasts are significantly
362 more reliable than the other weather center's ensembles for most lead times. The BS
363 shows that the ECMWF has the best, while the UKMO has the second-best performance.
364 From the BS and slopes of the reliability diagrams, the multi-model ensemble
365 shows relatively good skill compared to the single-center ensemble forecasts for almost
366 all lead times. The construction of multi-model ensembles can improve reliability
367 throughout the forecast periods. The MME plots nearly diagonally at lead times of two to
368 four days, while showing improved forecast skill for the ramp events for all lead times
369 compared with the single model.
370 The improvement in wind ramp forecasts using the multi-model ensemble can be
371 attributed to the increase in ensemble spread. A particular single-center forecast cannot
372 always show the best performance in predicting ramp events, since the ensemble forecasts
373 are occasionally very different. If some forecasts show high occurrence probabilities of

ramp events, the other single-center ensemble forecasts do not necessarily show similarly high probabilities. In this case, the MME will result in low probabilities of occurrence. However, if most of the models are in good agreement regarding the occurrence of ramp events, it can lead to the improvement of reliability with high forecast probabilities.

In addition to the effect of multi-model ensemble, we have also shown the effect of the analog ensemble. The results of the single ensemble method for the JMA ensemble forecasts and single-control forecast are presented in Fig. 10. To evaluate the skill of the hybrid ensemble forecasts, we have also shown the forecast skill obtained from the conventional (non-hybrid) scheme, namely, the nearest-neighbor single analog method. The single analog method was carried out for comparing the results obtained from only one single analog dataset (MME 1 analog). Instead of the use of SOM method, MME 1 analog predicted by picking up the reconstructed wind power data corresponding with the highest similarity in the atmospheric variables among the reanalysis data. We used Euclidean distance to measure similarity of the weather pattern and pick up one WP presenting the highest similarity. We compared the results obtained from the MME 1 analog for the JMA forecast and the full MME.

The resulting RMSE increases with increasing forecast lead time for all approaches, as shown in Fig. 10a. We see a relative improvement in RMSE when using the multi-model ensembles. Interestingly, the difference in RMSE of the median between the SOM analog ensemble and the single ensemble is very small. This seems to be related to a decrease in the number of valid analogs near the outer edge of the weather attractor. Appropriate analog numbers are considered to be different from one time to another.

Compared to RMSE, the prediction accuracy tends to be better in the analog ensemble method in CRPS (Fig. 10b). Despite the decrease in computational cost, the SOM-based analog ensemble method improves the skill versus conventional methods. This change could be attribute to the effect of the analog ensemble, which makes a more realistic forecasted PDF by obtaining nearby sample points.

4. Discussion and conclusions

In addition to evaluating the wind power potential [35], forecasting the variability of wind power is one of most important challenges in the energy sector [1]. In this study, we present the application of a SOM-based analog ensemble method for medium-range wind power generation/variation forecasts by using multi-center ensemble forecast data, to support system operation for transmission grid operators. As discussed in a previous study of wind power and climate in Japan [12], the wind ramp events in East Japan are largely affected by synoptic circulation. Most ramp-up events in Japan are due to approaching extra-tropical cyclones, while most ramp-downs are due to reduced gradients of surface pressure corresponding to the cover of anticyclonic highs. The complex relationships between synoptic-scale WPs and regionally integrated wind power generation were studied to obtain synoptic scale weather information around Japan by SOMs. We have shown the applications of the SOM, not only for analyzing multi-model ensemble forecasts, but also for the probabilistic forecasting of wind power generation and ramp events. The skill of the wind power forecasts based on the hybrid multi-model analog ensemble method using SOM was evaluated for the Tohoku region in East Japan. From

418 the results, we showed that regionally-integrated wind power production and variability,
419 in relation to synoptic-scale WPs, can be predicted days in advance. The medium-range
420 wind power forecast over Japan is relatively skillful. The skill predictability of multi-
421 center ensembles improves that of single-center ensembles significantly when using the
422 perfect prognosis approach. We confirmed that the SOM-compressed analog ensemble
423 improves the forecasts and can then be an effective estimation method when a very large
424 number of ensemble members (i.e., multi-center ensemble) and historical local data are
425 used. The information obtained about predictive uncertainty can be fruitful as an
426 information source for decision-making in transmission grid operation.

427 The multi-model ensemble surpasses that of the single-model for both deterministic
428 and probability forecasts [36]. As the multi-center ensemble cancels individual systematic
429 errors in each model, it can provide more realistic estimates than individual forecast
430 systems [37,38]. Since the hybrid ensemble method presented in this study needs SOM
431 analysis in advance, it is computationally expensive and complicated method. However,
432 this method can be an alternative method when we cannot use long-term wind power data.
433 The hybrid ensemble method presented in this study have a potential to provide more
434 realistic PDF. Moreover, it can be employed rapidly, with a very large number of
435 ensemble forecasts outputs from medium-range (weekly) to long-range (seasonal). While
436 it cannot include various feedback processes at a local scale, our method is particularly
437 advantageous from a computational cost perspective, as it quickly provides a first-order
438 estimation of weather impacts on regional wind power resources.
439

Acknowledgements

This research was supported by the "Research and development projects on power system output fluctuation-related technology" of the New Energy and Industrial Technology Development Organization (NEDO). The authors express their gratitude to the Ogimoto Lab at the Institute of Industrial Science, the University of Tokyo for providing the observed area-integrated wind power generation data, derived from a collaborative research project between the lab and the Japan Wind Power Association (JWPA). Part of this work was supported by the JSPS KAKENHI Grant Number JP 17K18426.

References

1. Marquis, M.; Wilczak, J.; Ahlstrom, M.; Sharp, J.; Stern, A.; Smith, J.C.; Calvert, S. Forecasting the wind to reach significant penetration levels of wind energy. *Bull. Amer Meteor Soc.* **2011**, 92, 1159–1171.

2. Lorenz, E.N. Atmospheric predictability as revealed by naturally occurring analogs. *J Atmos Sci*. **1969**, 26, 639–646.

3. Zorita, E.; von Storch, H. The analog method as a simple statistical downscaling technique: comparison with more complicated methods. *J. Clim.* **1999**, 12, 2474–2489.

4. Timbal, B.; McAvaney, B.J. An analogue-based method to downscale surface air temperature: application for Australia. *Clim. Dyn.*. **2001**, 17, 947–963.

5. Gutierrez, J.M.; Cofino, A.S.; Cano, R.; Sordo, C. Analysis and downscaling multi-model seasonal forecasts in Peru using self-organizing maps. *Tellus A.* **2005**, 57, 435–447.

6. Garcia-Morales, M.B.; Dubus, L. Forecasting precipitation for hydroelectric power management: how to exploit GCM's seasonal ensemble forecasts. *Int J Climatol*. **2007**, 27, 1691–1705.

7. Delle Monache, L.; Eckel, T.; Rife, D.; Nagarajan, B. Probabilistic weather prediction with an analog ensemble. *Mon Wea Rev.* **2013**, 141, 3498–3516.

8. Kohonen, T. Self-organized formation of topologically correct feature maps. *Biological Cybernetics.* **1982**, 43, 59–69.

9. Hewitson, B.C.; Crane, R.G. Consensus between GCM climate change projections with empirical downscaling: precipitation downscaling over South Africa. *Int J Climatol*. **2006**, 26, 1315–1337.

10. Borah, N.; Sahai, A.K.; Chattopadhyay, R.; Joseph, S.; Abhilash, S. et al. Self-organizing map-based ensemble forecast system for extended range prediction of active/break cycles of Indian summer monsoon. *J Geophy Res Atmos*. **2013**, 118, 1–13.

11. Ohba, M.; Nohara, D.; Kadokura, S.; Toyoda, Y. Rainfall Downscaling of Weekly Ensemble Forecasts using Self-Organizing Maps. *Tellus A*. **2016**, 68, 29293. doi: 10.3402/tellusa.v68.29293.

12. Ohba, M.; Nohara, D.; Kadokura, S. Impacts of Synoptic Circulation Patterns on Wind Power Ramp Events in East Japan. *Renewable Energy.* **2016**, 96, 591–602.

13. Kobayashi, S.; Ota, Y.; Harada, Y.; Ebita, A.; Moriya, M.; Onoda, H. et al. The JRA-55 Reanalysis: General specifications and basic characteristics. *J Meteor Soc Japan* **2015**, 93, 5–48.

14. Ohba. M.; Kadokura, S.; Nohara, D.; Toyoda, Y. Anomalous Weather Patterns in Relation to Heavy Precipitation Events in Japan during the Baiu Season. *Journal of Hydrometeorology*. **2015**, 16, 688–701.

15. Reusch, D.B.; Alley, R.B.; Hewitson, B.C. North Atlantic climate variability from a self-organizing map perspective. *J Geophys Res.* **2007**, 112, D02104. doi: 10.1029/2006JD007460.

16. Ito, M.; Miyoshi, T.; Masuyama, H. The characteristics of the torus self-organizing map. Proc 16th Fuzzy System Symp Akita Japan Society for Fuzzy and Systems **2000**, 373–374.

17. Alessandrini, S.; Delle Monache, L.; Sperati, S.; Nissen, J. Short-term wind power forecasting with an analog ensemble. *Renewable Energy.* **2015**, 76, 768–781.

18. Vanvyve, E.; Delle Monache, L.; Monaghan, A.J.; Pinto, J. Wind resource estimates with an analog ensemble approach. *Renewable Energy.* **2015**, 74, 761–773.

19. Eckel, F.A.; Delle Monache, L. A hybrid NWP-analog ensemble. *Monthly Weather Review*. **2016**, 144, 897–911.

20. Klink, K. Atmospheric circulation effects on wind speed variability at turbine height. *J Appl Meteorol Climatol*. **2007**, 46, 445–456.

21. Cutler, N.J.; Outhred, H.R.; MacGill, I.F.; Kepert, J.D. Predicting and presenting plausible future scenarios of wind power production from numerical weather prediction systems: a qualitative ex ante evaluation for decision making. *Wind Energy* **2012**, 15, 473–488.

22. Hamlington, B.D.; Hamlington, P.E.; Collins, S.G.; Alexander, S.R.; Kim, K.Y. Effects of climate oscillations on wind resource variability in the United States.

509 *Geophys Res Lett*. **2015**, 42, 145–152.

510 23. Gibson, P.B.; Cullen, N.J. Synoptic and sub-synoptic circulation effects on wind
511 resource variability – A case study from a coastal terrain setting in New Zealand.
512 *Renewable Energy.* **2015**, 78, 253-263, doi:10.1016/j.renene.2015.01.004.

513 24. Pryor, S.C.; Schoof, J.; Barthelmie, R.J. The impact of non-stationarities in the
514 climate system on the definition of a 'normal wind year': A case study from the Baltic.
515 *Int J Climatol*. **2005**, 25, 735–752.

516 25. Davy, R.; Milton, J.; Russel, C.; Coppin, P. Statistical downscaling of wind variability
517 from meteorological fields. *Bound Layer Meteorol.* **2010**, 135, 165-175.

518 26. Peña, J.C.; Aran, M.; Cunillera, J.; Amaro, J. Atmospheric circulation patterns
519 associated with strong wind events in Catalonia. *Nat. Hazards Earth Syst Sci*. **2011**,
520 11, 145–155.

521 27. Brayshaw, D.J.; Troccoli, A.; Fordham, R.; Methven, J. The impact of large scale
522 atmospheric circulation patterns on wind power generation and its potential
523 predictability: a case study over the UK. *Renewable Energy.* **2011**, 36, 2087–2096.

524 28. Ely, C.R.; Brayshaw, D.J.; Methven, J.; Cox, J.; Pearce, P. Implications of the North
525 Atlantic Oscillation for a UK-Norway renewable power system. *Energy Policy*. **2013**,
526 62, 1420–1427.

527 29. Deppe, A.J.; Gallus, W.A.; Takle, E.S. A WRF ensemble for improved wind speed
528 forecasts at turbine height. *Wea Forecasting*. **2013**, 28, 212–228.

30. Marshall, A.G.; Hudson, D.; Hendon, H.H.; Pook, M.J.; Alves, O.; Wheeler, M.C. Simulation and prediction of blocking in the Australian region and its influence on intra-seasonal rainfall in POAMA-2. *Clim Dyn.* **2014**, 42, 3271–3288.

31. Hudson, D.; Alves, O.; Hendon, H.H.; Marshall, A.G. Bridging the Gap between Weather and Seasonal Forecasting: Intraseasonal Forecasting for Australia. *Q J R Meteor Soc.* **2011**, 137, 673–689.

32. White, C.J.; Hudson, D.; Alves, O. ENSO, the IOD and the intraseasonal prediction of heat extremes across Australia using POAMA-2. *Clim Dyn*. **2014**, 43, 1791–1810.

33. Johnson, N.C.; Collins, D.C.; Feldstein, S.B.; L'Heureux, M.L.; Riddle, E.E. Skillful wintertime North American temperature forecasts out to four weeks based on the state of ENSO and the MJO. *Wea Forecasting*. **2014**, 29, 23–38.

34. Hersbach, H. Decomposition of the continuous ranked probability score for ensemble prediction systems. *Wea. Forecasting*. **2000**, 15, 559–570.

35. Archer, C.L.; Jacobson, M.Z. Evaluation of global wind power. *J Geophys Res Atmos*. **2005**, 110, D12110.

36. Park, Y.Y.; Buizza, R.; Leutbecher, M. TIGGE: Preliminary results on comparing and combining ensembles. *Q J R Meteorol Soc*. **2008**, 134, 2051–2066.

37. Matsueda, M., Tanaka, H.L. Can MCGE outperform the ECMWF ensemble? *SOLA*. **2008**, 4, 77–80.

549 38. Johnson, C.; Swinbank, R. Medium-range multimodel ensemble combination and
550 calibration. *Q J Roy Meteorol Soc*. **2009**, 135, 777–794.

551 39. Gibson, P.B.; Cullen, N.J. Regional variability in New Zealand's wind resource
552 linked to synoptic-scale circulation: implications for generation reliability. *Journal*
553 *of Applied Meteorology and Climatology.* **2015**, 54, 944-958.

554 40. International Energy Agency World energy outlook: 2016. *OECD/IEA.* **2016**, 684.

555 41. Junk, C.; Delle Monache, L.; Alessandrini, S.; von Bremen, L.; Cervone, G.
556 Predictor-weighting strategies for probabilistic wind power forecasting with an
557 analog ensemble. *Meteorologische Zeitschrift.* **2015**, 24, 361-379.

558 42. Davò, F.; Alessandrini, S.; Sperati, S.; Delle Monache, L.; Airoldi, D.; Vespucci, M.T.
559 Post-processing techniques and principal component analysis for regional wind
560 power and solar irradiance forecasting. *Solar Energy.* **2016**, 134, 327-338.

List of Figures

583 Each bottom-left figure show the correspondence with Figs. 3a-c, respectively.
584 (b) SOM frequency (best-matched) of the 168 multi-center ensemble members
585 on the 50 x 50 SOM lattice for forecast days 1–8 initiated from 1st January 2013.
586 Solid black box represents the actual state.
587
588 Figure. 5. Forecasted 6-h wind power forecasts obtained from the single center ensembles
589 with SOM-based analog-ensemble, initiated from (a) 13th February 2012, (b) 1st
590 January 2013, and (c) 2nd February 2013, at 12:00 UTC, as examples of the
591 forecast results. Red line represents the observed wind power generation. PDFs
592 of wind power generation obtained from the hybrid ensemble are represented by
593 green shading. Gray line represents median values of each ensemble member
594 (total 168 lines). Each figure at the bottom shows the forecasted ramp probability
595 obtained from the SOM nodes and the medians of each ensemble are represented
596 by red and blue bars and dots, respectively, with the error bar. Observed ramp up
597 and ramp down events (actual state) are represented by the red and blue lines,
598 respectively.
599
600 Figure. 6. Same as Fig. 5, except it is obtained from the five single-center ensembles with
601 SOM-based analog-ensemble initiated from 1st January 2013, at 12:00 UTC.
602
603 Figure. 7. Forecasted 6-h wind power generation obtained from the hybrid ensemble for
604 2-day, 3-day, 5-day, and 7-day forecasts around 1st January 2013. Black line

605 represents the observed wind power generation. Forecasted PDFs of wind power
606 generation obtained from the hybrid ensemble are represented by green shading.
607 Each figure at the bottom shows the forecasted ramp probability obtained from
608 the SOM nodes and the medium of each ensemble, represented by red and blue
609 bars and dots, respectively. Observed ramp up and ramp down events (actual
610 state) are represented by the red and blue lines, respectively.
611
612 Figure. 8. (a) RMSE, (b) continuous ranked probability score, and (c) Brier score for wind
613 power generation forecasts by CMC (orange), ECMWF (blue), JMA (red),
614 NCEP (green), UKMO (purple), and MME (black) for the targeted region from
615 Apr 2011 to May 2013.
616
617 Figure. 9. Reliability diagrams for 2-day, 4-day, and 6-day forecasts of wind ramp events
618 in the Tohoku region from Apr 2011 to May 2013, obtained from the MME and
619 five single-center ensembles. Frequency histograms are represented by gray bars
620 and dot colors.
621
622 Figure. 10. Same as Fig.8a and 8b, except for wind power generation forecasts, using
623 single analog method for MME (gray). JMA (red) and MME (black) are the same
624 as in Fig. 8.
625

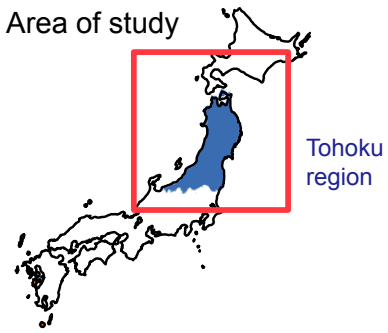

Fig. 1. Area of study in East Japan (red solid box) used to define the atmospheric patterns. The blue shading represents the Tohoku region (served by Tohoku Electric Power Co., Inc.), Japan.

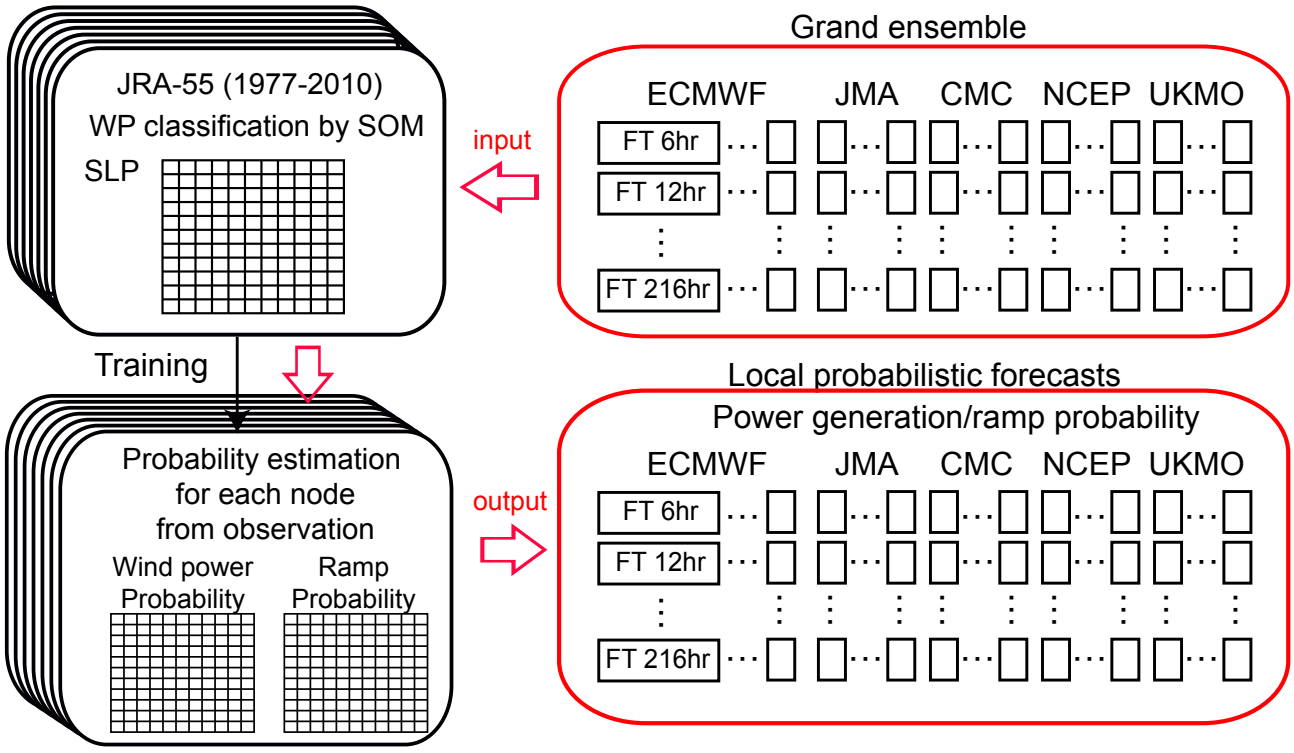

FIG. 2. Schematic diagram of the hybrid ensemble by using SOM. The multiple different SOM classifications of the WP are based on the three atmospheric variables during 1977-2011 (top left). Based on the SOM lattices, the PDF of wind power generation and ramp probability are estimated for each node (bottom left). By using the SOM lattice, the forecasted wind power generation and variation are obtained (bottom right) from the 168 members of the multi center ensemble forecasts (top right).

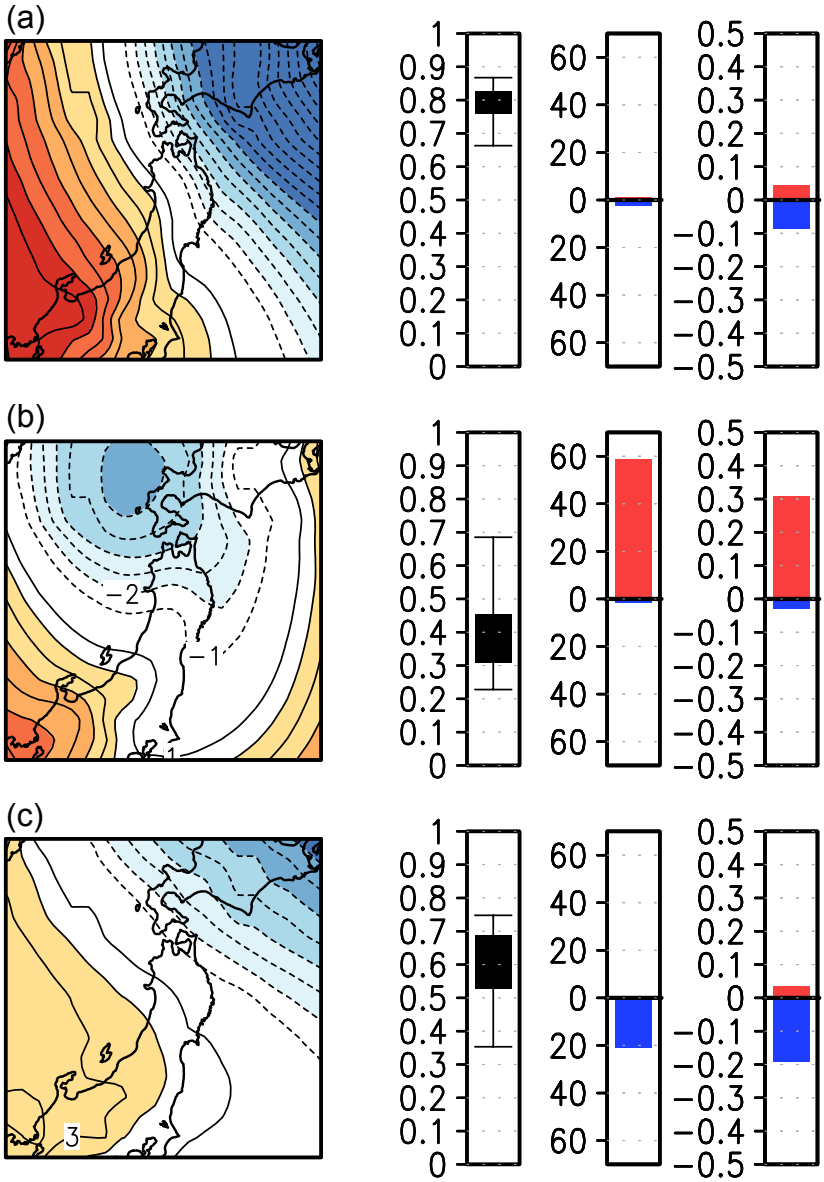

FIG. 3. (a)-(c) Three examples of WPs (SLP) derived from the 50 x 50 SOM non-linear classification (hPa: red and blue shading). Right panels show the WP-related wind power generation (p.u. black error bar for 5th, 25th, 75th and 95th percentiles) frequency occurrence rate (%) of ramp-up (red) and down (blue), and maximum up (red) and down (blue) of wind power generation (p.u.) over a period ≤ 6 hours for each SOM node.

Preprints (www.preprints.org) | NOT PEER-REVIEWED | Posted: 20 September 2018 doi:10.20944/preprints201809.0404.v1

Peer-reviewed version available at Atmosphere 2018, 9, 423; doi:10.3390/atmos9110423

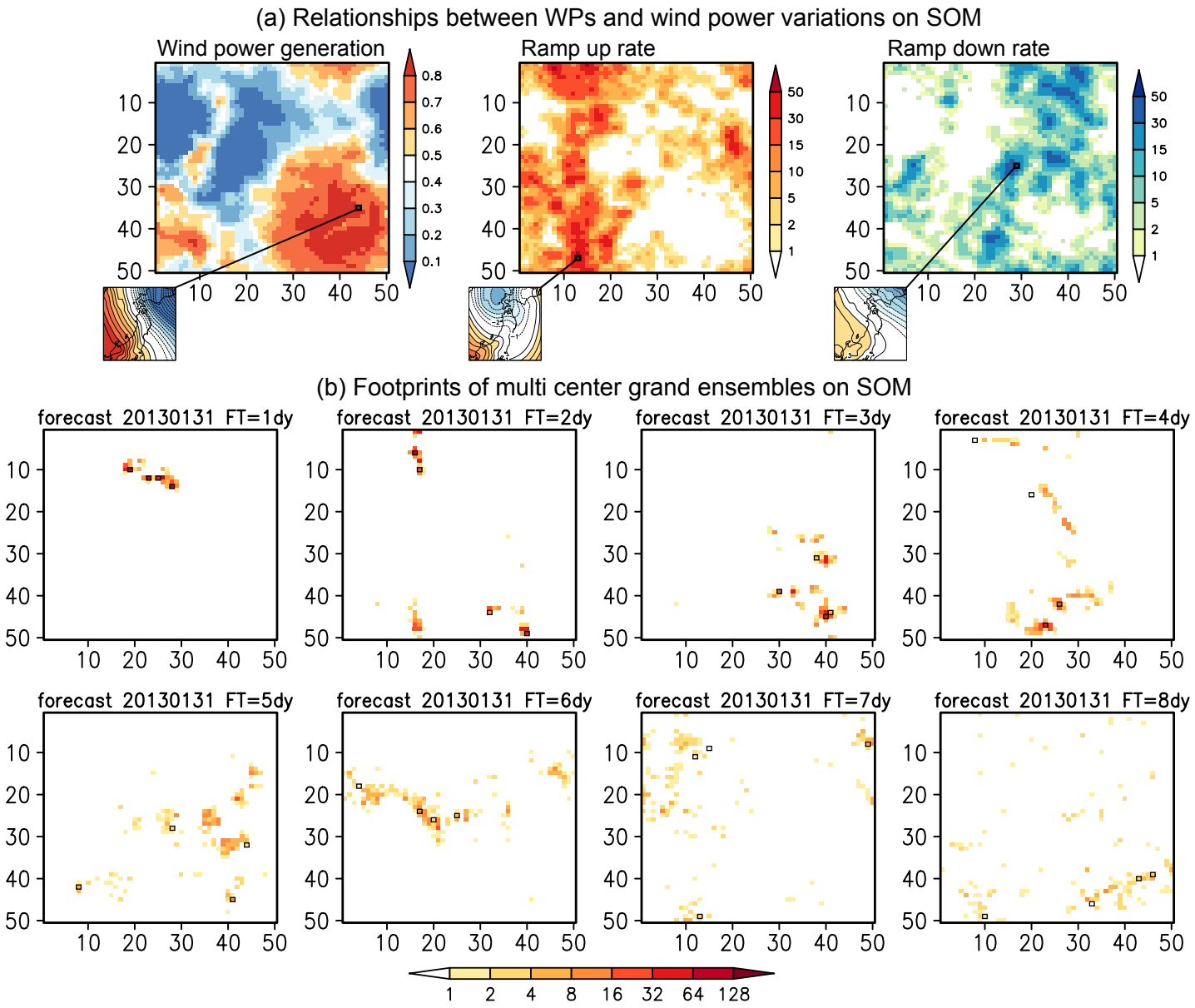

Fig. 4. (a) The median values of wind power generation (left), frequency occurrence rate (%) of ramp-up (middle) and ramp-down (right) within each SOM node. Each bottom-left figures show the correspondence with Fig. 3a-c, respectively. (b) SOM frequency (best-matched) of the 168 multi-center ensemble members on the 50 x 50 SOM lattice for forecast days 1–8 initiated from 1st January 2013. Solid black box represents the actual state.

Preprints (www.preprints.org) | NOT PEER-REVIEWED | Posted: 20 September 2018 doi:10.20944/preprints201809.0404.v1

Peer-reviewed version available at Atmosphere 2018, 9, 423; doi:10.3390/atmos9110423

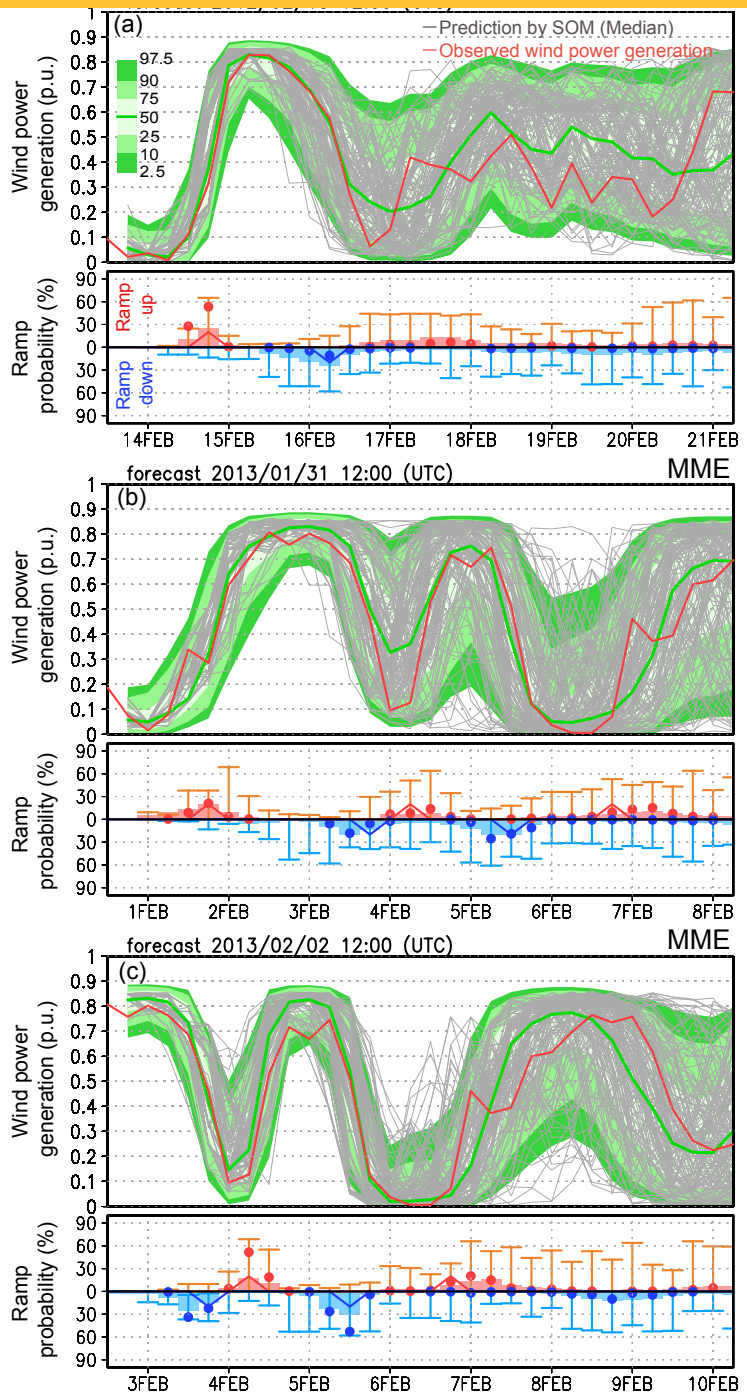

FIG. 5. Forecasted 6-h wind power forecasts obtained from the single center ensembles with SOM-based analog-ensemble initiated from (a) 13 February 2012, (b) 1 January 2013, and (c) 2 February 2013 12:00 UTC as examples of the forecast results. Red line represents the observed wind power generation. PDFs of wind power generation obtained from the hybrid ensemble are represented by green shading. Each bottom figure shows the forecasted ramp probability obtained from the SOM nodes (medium of each ensemble) are represented by red and blue bars (dots) with the error bar. Observed ramp up and ramp down events (actual state) is represented by the red and blue lines, respectively.

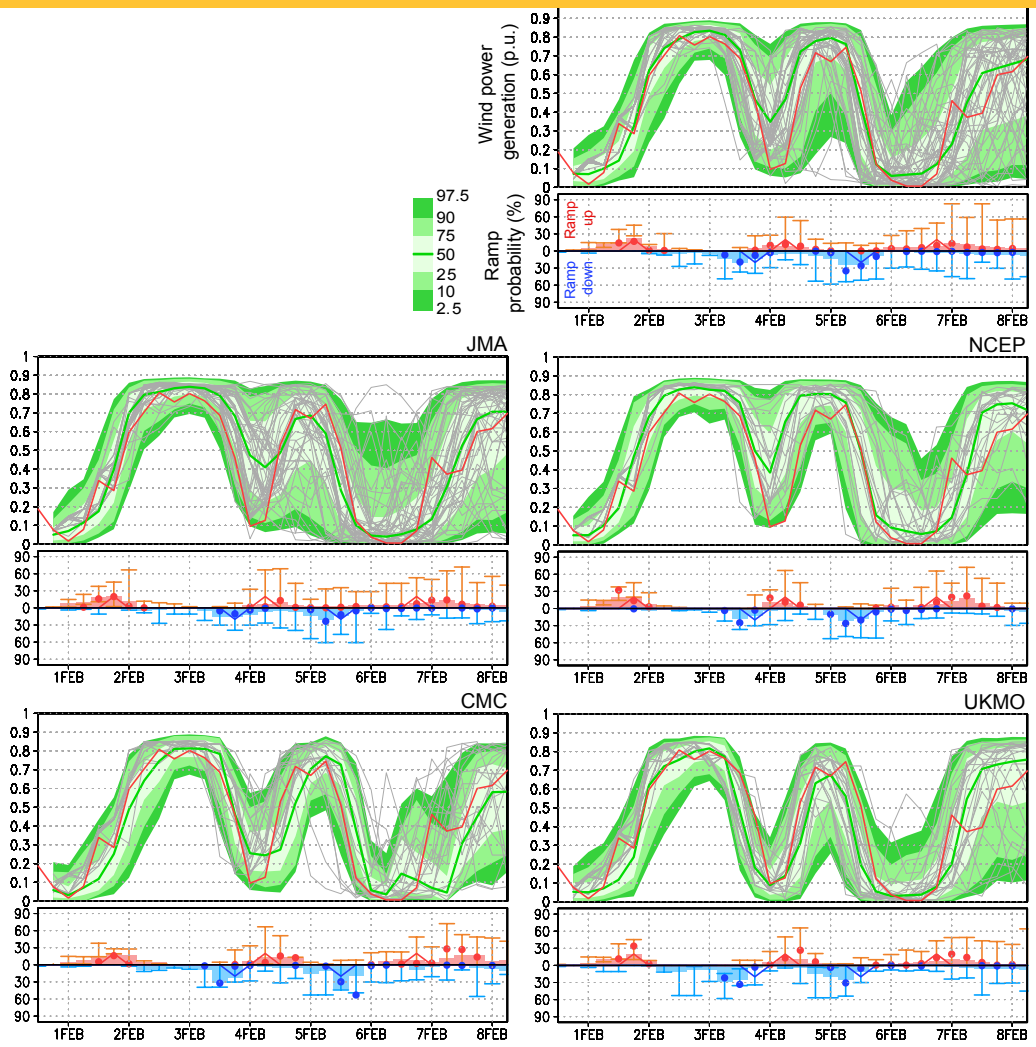

FIG. 6. Same as Fig. 5 except for that is obtained from the five single-center ensembles with SOM-based analog-ensemble initiated from 1 January 2013 12:00 UTC.

Preprints (www.preprints.org) | NOT PEER-REVIEWED | Posted: 20 September 2018 doi:10.20944/preprints201809.0404.v1

Peer-reviewed version available at Atmosphere 2018, 9, 423; doi:10.3390/atmos9110423

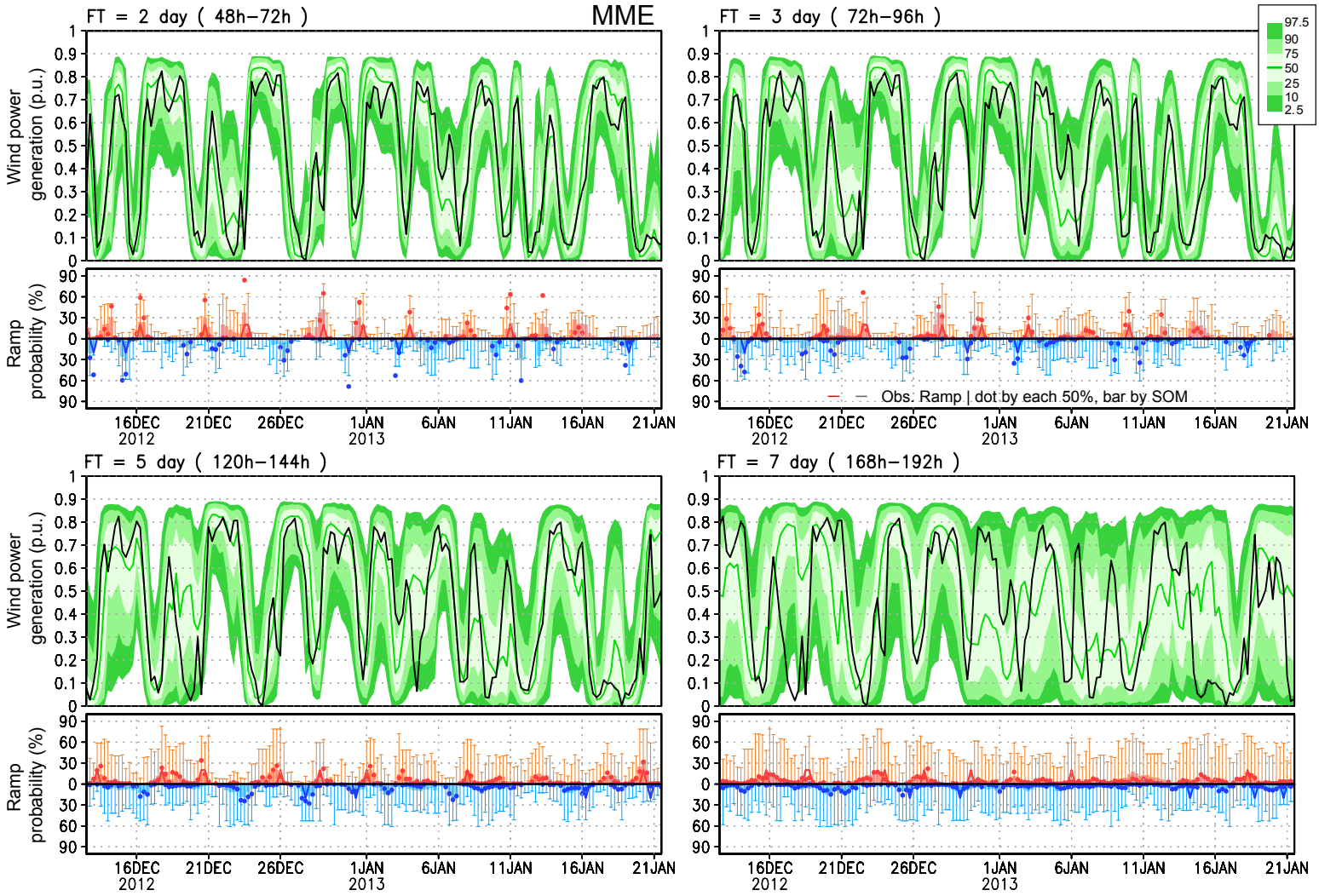

FIG. 7. Forecasted 6-h wind power generation obtained from the hybrid ensemble for 2-day, 3-day, 5-day, and 7-day forecasts around 1 January 2013. Black line represents the observed wind power generation. Forecasted PDFs of wind power generation obtained from the hybrid ensemble are represented by green shading. Each bottom figure shows the forecasted ramp probability obtained from the SOM nodes (medium of each ensemble), represented by red and blue bars (dots). Observed ramp up and ramp down events (actual state) is represented by the red and blue lines, respectively.

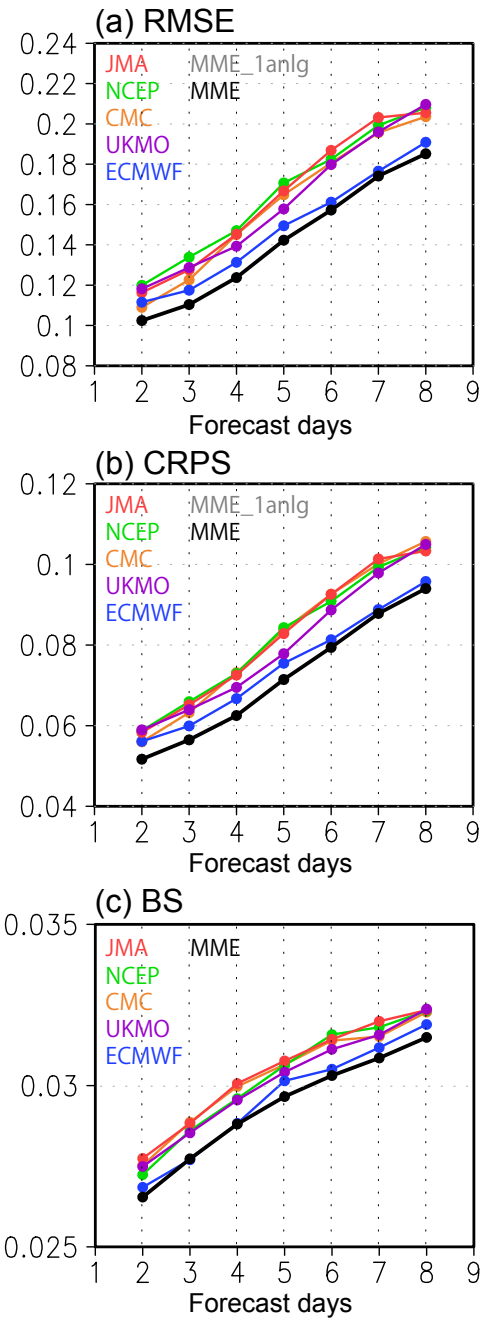

FIG. 8. (a) Root mean square error, (b) continuous ranked probability score, and (c) Brier score for wind power generation forecasts by CMC (orange), ECMWF (blue), JMA (red), NCEP (green), UKMO (purple), and MME (black) for the targeted region from Apr 2011 to May 2013.

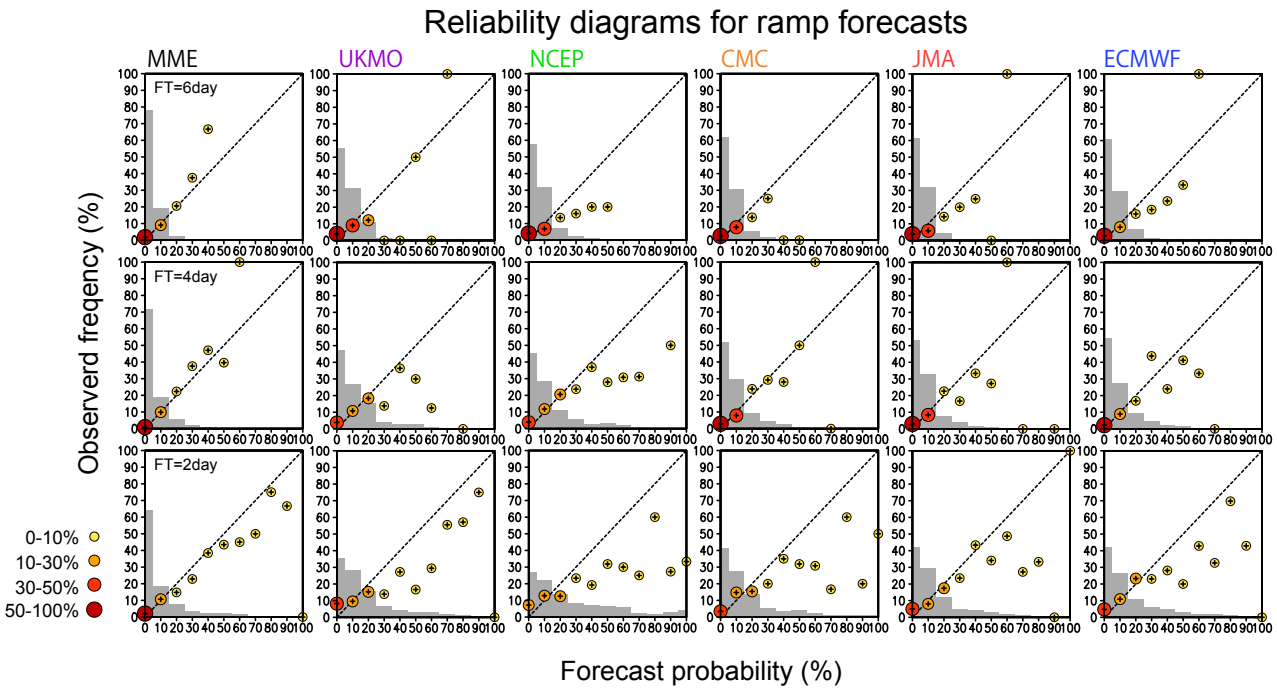

FIG. 9. Reliability diagrams for 2-day, 4-day, and 6-day forecasts of wind ramp events in the Tohoku region from Apr 2011 to May 2013 obtained from the MME and five single-center ensembles.

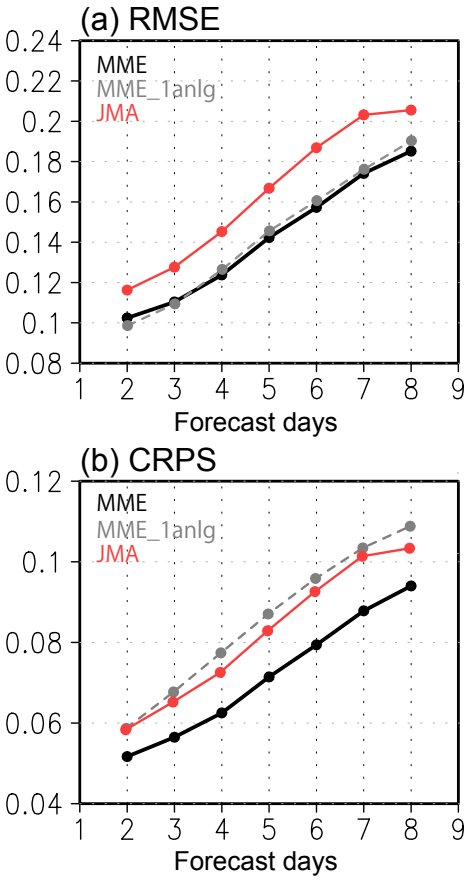

Fig. 10. Same as Fig.8a and 8b, except for wind power generation forecasts, using single analog method for MME (gray). JMA (red) and MME (black) are the same as in Fig. 8.